

Interaction of Palladium(II) and Platinum(II) Complexes with Microperoxidase-11 Studied by Electrospray Mass Spectrometry and MS/MS Analysis

Xiaojuan Sun, Chen Jin, Yuhua Mei, Gaosheng Yang, Zijian Guo, and Longgen Zhu*

State Key Laboratory of Coordination Chemistry, Coordination Chemistry Institute, Nanjing University, Nanjing 210093, China

Received May 10, 2003

Interactions of *cis*-[Pd(en)(H₂O)₂]²⁺ (en, ethylenediamine) and *cis*-[Pt(NH₃)₂(H₂O)₂]²⁺ with microperoxidase-11 (MP-11) in a molar ratio of 1:1 or 2:1 at pH 1.4 were investigated via electrospray mass spectrometry and MS/MS analysis at room temperature and at 40 °C with an incubation time of 2 or 3 days. The composition of the Pd(II)- and Pt(II)-anchored MP-11 was confirmed on the basis of the precise molecular mass and the simulated isotope distribution pattern. MS/MS analysis revealed that the Pd(II) center anchored to the side chain of Cys7 as Pd(II) and MP-11 were mixed in an equimolar ratio and to side chains of Cys7 and Cys4 as Pd(II) and MP-11 mixed in a 2:1 molar ratio. When Pt(II) and MP-11 were mixed in a 2:1 molar ratio, Pt(II) first anchored to the side chain of Cys7, and then to the side chain of Cys4 with time. The initial coordination of Pd(II) and Pt(II) to the side chain of Cys7 is the essential step for the Pd(II)- and Pt(II)-promoted cleavage of the His8–Thr9 bond in MP-11. These results support the hypothesis that the Pd(II)-mediated cleavage of the His18–Thr19 bond in cytochrome *c* is due to the identical binding mode.

Introduction

In recent years, a variety of metal complexes have been used as “inorganic proteases” to cleave the peptide bonds in peptides and proteins.^{1–4} These metal complexes included are Co(II, III) complexes,^{5,6} Fe-EDTA derivative,^{7–9} CuCl₂^{10–12} and its macrocyclic complex,¹³ Ce(IV) complex,^{14,15} ZnCl₂,¹⁶

Pd(II),^{17–35} and Pt(II) complexes.^{36–38} These complexes can cleave short peptides and proteins hydrolytically and selec-

* Author to whom correspondence should be addressed. E-mail: Zhulg@public1.ptt.js.cn.

- (1) Probing of Proteins by Metal Ions and Their Low-Molecular-Weight Complexes. *Metal Ions in Biological System*; Sigel, A., Sigel, H., Eds.; Dekker: New York, 2001; Vol. 38, Chapters 2–9.
- (2) Hegg, E. L.; Burstyn, J. N. *Coord. Chem. Rev.* **1998**, *173*, 133.
- (3) Suh, J. *Acc. Chem. Res.* **1992**, *25*, 273.
- (4) Chin, J. *Acc. Chem. Res.* **1991**, *24*, 145.
- (5) Sutton, P. A.; Buckingham, D. A. *Acc. Chem. Res.* **1987**, *20*, 357.
- (6) Kumar, C. V.; Buranaprapuk, A.; Cho, A.; Chaudhari, A. *Chem. Commun.* **2000**, 597.
- (7) Rana, T. M.; Meares, C. F. *J. Am. Chem. Soc.* **1990**, *112*, 2457.
- (8) Rana, T. M.; Meares, C. F. *J. Am. Chem. Soc.* **1991**, *113*, 1859.
- (9) Rana, T. M.; Meares, C. F. *Proc. Natl. Acad. Sci. U.S.A.* **1991**, *88*, 10578.
- (10) Allen, G.; Campbell, R. O. *Int. J. Pept. Protein Res.* **1996**, *48*, 265.
- (11) Zhang, L.; Mei, Y.; Zhang, Y.; Li, S.; Sun, X.; Zhu, L. *Inorg. Chem.* **2003**, *42*, 492.
- (12) Luo, X.; He, W.; Zhang, Y.; Guo, Z.; Zhu, L. *Chin. J. Chem.* **2000**, *18*, 855.
- (13) Hegg, E. L.; Burstyn, J. N. *J. Am. Chem. Soc.* **1995**, *117*, 70.
- (14) Yashiro, M.; Takarada, T.; Miyama, S.; Komiyama, M. *J. Chem. Soc., Chem. Commun.* **1994**, 1757.

- (15) Takarada, T.; Yashiro, M.; Komiyama, M. *Chem. Eur. J.* **2000**, *6*, 3906.
- (16) Yashiro, M.; Sonobe, Y.; Yamamura, A.; Takarada, T.; Komiyama, M. *Org. Biomol. Chem.* **2003**, *1*, 629.
- (17) Zhu, L.; Kostić, N. M. *Inorg. Chem.* **1992**, *31*, 3994.
- (18) Zhu, L.; Kostić, N. M. *J. Am. Chem. Soc.* **1993**, *115*, 4566.
- (19) Zhu, L.; Kostić, N. M. *Inorg. Chim. Acta* **1994**, *21*, 721.
- (20) Chen, X.; Zhu, L.; Yan, H.; You, X.; Kostić, N. M. *J. Chem. Soc., Dalton Trans.* **1996**, 2653.
- (21) Chen, X.; Zhu, L.; You, X.; Kostić, N. M. *J. Biol. Inorg. Chem.* **1998**, *3*, 1.
- (22) Chen, X.; Luo, X.; Song, Y.; Zhou, S.; Zhu, L. *Polyhedron* **1998**, *17*, 2271.
- (23) Parac, T. N.; Kostić, N. M. *J. Am. Chem. Soc.* **1996**, *118*, 51.
- (24) Parac, T. N.; Kostić, N. M. *J. Am. Chem. Soc.* **1996**, *118*, 5946.
- (25) Karet, G. B.; Kostić, N. M. *Inorg. Chem.* **1998**, *37*, 1021.
- (26) Parac, T. N.; Ullmann, G. M.; Kostić, N. M. *J. Am. Chem. Soc.* **1999**, *121*, 3127.
- (27) Luo, X.; He, W.; Zhang, Y.; Guo, Z.; Zhu, L. *Chem. Lett.* **2000**, *18*, 855.
- (28) Milović, N. M.; Kostić, N. M. *Inorg. Chem.* **2002**, *41*, 7053.
- (29) Milović, N. M.; Kostić, N. M. *J. Am. Chem. Soc.* **2002**, *124*, 4759.
- (30) Milović, N. M.; Kostić, N. M. *J. Am. Chem. Soc.* **2003**, *125*, 781.
- (31) Sun, X.; Zhang, L.; Zhang, Y.; Yang, G.; Guo, Z.; Zhu, L. *New J. Chem.* **2003**, *27*, 818.
- (32) Zhu, L.; Qin, L.; Parac, T. N.; Kostić, N. M. *J. Am. Chem. Soc.* **1994**, *116*, 5218.
- (33) Zhu, L.; Bakhtiar, R.; Kostić, N. M. *J. Biol. Inorg. Chem.* **1998**, *3*, 383.

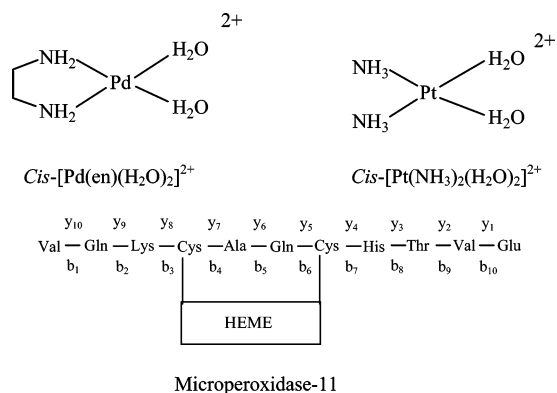
tively and mimic aminopeptidases and endopeptidases. Although great progress has been made, little is known about the mechanisms which govern the site of cleavage. These are very important for understanding the nature of peptide bond cleavage with metal complexes and for designing new cleaved reagents. Previous studies showed that horse heart cytochrome *c* (Cyt *c*) and its apocytochrome *c* were specifically cleaved at the His18–Thr19 bond in the presence of an equimolar amount or a small excess of the Pd(II) complexes at 40 °C.^{32,34} The site of cleavage was confirmed by the N-terminal amino acid sequencing and electrospray mass spectrometry (ESIMS) for a bigger cleaved fragment. Besides the site of cleavage, the additional sites of cleavage were recently identified under a more forcing condition, using a 10-fold molar excess of the Pd(II) complex for incubation at 60 °C.²⁸ Different from the His18–Thr19 bond cleavage that is downstream from His18, the other sites of cleavage are second peptide bond upstream from Met65, Met80, His26, and His33. Although the difference in cleaving sites was explained in some detail in ref 28, the evidence was absent. Therefore, the question of where the Pd(II) initially anchors is still open for further investigation.

As is known for the cytochrome *c* sequence, there are two *S*-alkylated cysteines, Cys14 and Cys17. The thioether groups of these residues provide potential binding sites for Pd(II) complexes, especially, the *S*-alkylated Cys17 precedes the His18. Although the cleaving site of the His18–Thr19 bond is clear now, we are not yet certain as to which residue (Cys17 or His18 or both) the Pd(II) ion initially anchors.^{1,28,31,32} There are two binding sites proposed which are associated with different mechanisms for the bond cleavage. One proposal is that the Pd(II) anchors to His18, then cleaves the His18–Thr19 bond^{1,28} (ref 1, page 180 in Chapter 5). The other proposal is that the Pd(II) initially anchors to Cys17 and then cleaves the His18–Thr19 bond.^{31,32} To clarify the question, in this work, a microperoxidase-11 (MP-11), which is a heme-containing fragment 11–21 of cytochrome *c*, was used for further investigating the initial interaction of the MP-11 with Pd(II) and Pt(II) complexes using ESIMS and MS/MS analysis. The results showed that MS/MS analysis is capable of determining the anchoring sites of Pd(II) and Pt(II) ions to MP-11.

Experimental Section

Double-distilled water was used for the preparation of solution. *cis*-[Pd(en)Cl₂] (en, ethylenediamine) and *cis*-[Pt(NH₃)₂Cl₂] were prepared using a published procedure.^{39,40} The corresponding diaqua complexes, shown in Chart 1, were obtained by treating them with 2.0 equiv of anhydrous AgBF₄ in H₂O and stirring at 35 °C for 4 h for *cis*-[Pd(en)Cl₂] and overnight for *cis*-[Pt(NH₃)₂Cl₂]. The white

Chart 1



solid AgCl was removed by centrifugation in the dark. The *cis*-[Pd(en)(H₂O)₂]²⁺ and *cis*-[Pt(NH₃)₂(H₂O)₂]²⁺ were freshly prepared prior to use. MP-11 in Chart 1 was obtained from Sigma and used without further treatment. Two peaks at 931 and 621 were observed in ESIMS that were assigned to two and three positively charged ions of MP-11. The MP-11 also contains some impurities, such as free heme (617). A mixed solution contained 40.0 μL of MP-11 (1.0 mg), 10.74 μL of *cis*-[Pd(en)(H₂O)₂]²⁺ or *cis*-[Pt(NH₃)₂(H₂O)₂]²⁺ (0.100 M) in a two molar excess over MP-11, 3.0 μL of 2.0 M HBF₄ for adjusting pH to ca. 1.4, and water to make the total volume up to 60.0 μL. The mixed solution was separated into two portions. One portion of 10 μL was kept at room temperature for 30 min for [Pd(en)(H₂O)₂]²⁺ or for 1 h for *cis*-[Pt(NH₃)₂(H₂O)₂]²⁺, and then used in ESIMS measurements. The rest of the solution was incubated at 40 °C for 2 or 3 days, respectively, and then used in ESIMS measurements.

ESIMS and MS/MS Analysis. Electrospray mass spectra were recorded on a model LCQ ion trap mass spectrometer (Finnigan) equipped with a HPLC and a Finnigan MAT electrospray ion source. 1.0 μL aliquots of mixed solution were directly injected to the MS detector for ESIMS analysis. The molecular masses were determined by transformation of ESIMS raw data into a true molecular mass scale using the software of Bioexplore.

For MS/MS analysis, the most intense ion in the spectra was selected as precursor ion, and a collision-induced dissociation scan with an isolation width of 3 *m/z* was performed with the relative collision energy 30 to optimize the fragmentation of the peptide. The employed voltage at the electrospray needles was 4.5 kV, and the heated capillary temperature was 200 °C.

Results and Discussion

ESIMS Measurement for the Mixed Solution of *cis*-[Pd(en)(H₂O)₂]²⁺ with MP-11. A solution of MP-11 and *cis*-[Pd(en)(H₂O)₂]²⁺ mixed in a molar ratio of 1:1 at pH 1.4 was kept at room temperature for 30 min and then measured by ESIMS. As shown in Figure 1, two new abundant peaks at 676.2 and 1012.9 were observed in addition to the peaks at 617.4 and 930.9 that are respectively attributed to free heme and MP-11. In Figure 1, the isotopic peaks of 676.2 separated by 0.3 *m/z* unit (A) fit very well to the isotope distribution pattern (B) calculated with the IsoPro 3.0 program for [C₈₆H₁₂₃FeN₂₂O₂₁S₂Pd+H⁺]³⁺. As shown in Figure 1C,D, the isotopic peaks of 1012.9 separated by 0.5 *m/z* unit, combined with the simulated isotope distribution pattern, are attributed to a double charged cationic complex of [C₈₆H₁₂₃FeN₂₂O₂₁S₂Pd]²⁺. Therefore, the peaks at 676.2

(34) Qiao, F.; Hu, J.; Zhu, H.; Luo, X.; Zhu, L.; Zhu, D. *Polyhedron* **1999**, *8*, 1629.

(35) Zhu, L.; Kostić, N. M. *Inorg. Chim. Acta* **2002**, *339*, 104.

(36) Burgeson, I. E.; Kostić, N. M. *Inorg. Chem.* **1991**, *30*, 4299.

(37) Hahn, M.; Kleine, M.; Sheldrick, W. S. *J. Biol. Inorg. Chem.* **2001**, *6*, 556.

(38) Milović, N. M.; Duteă, L.-M.; Kostić, N. M. *Inorg. Chem.* **2003**, *42*, 4036.

(39) Hohmann, H.; Van Eldik, R. *Inorg. Chim. Acta* **1990**, *174*, 87.

(40) Dhara, S. C. *Indian J. Chem.* **1970**, *8*, 193.

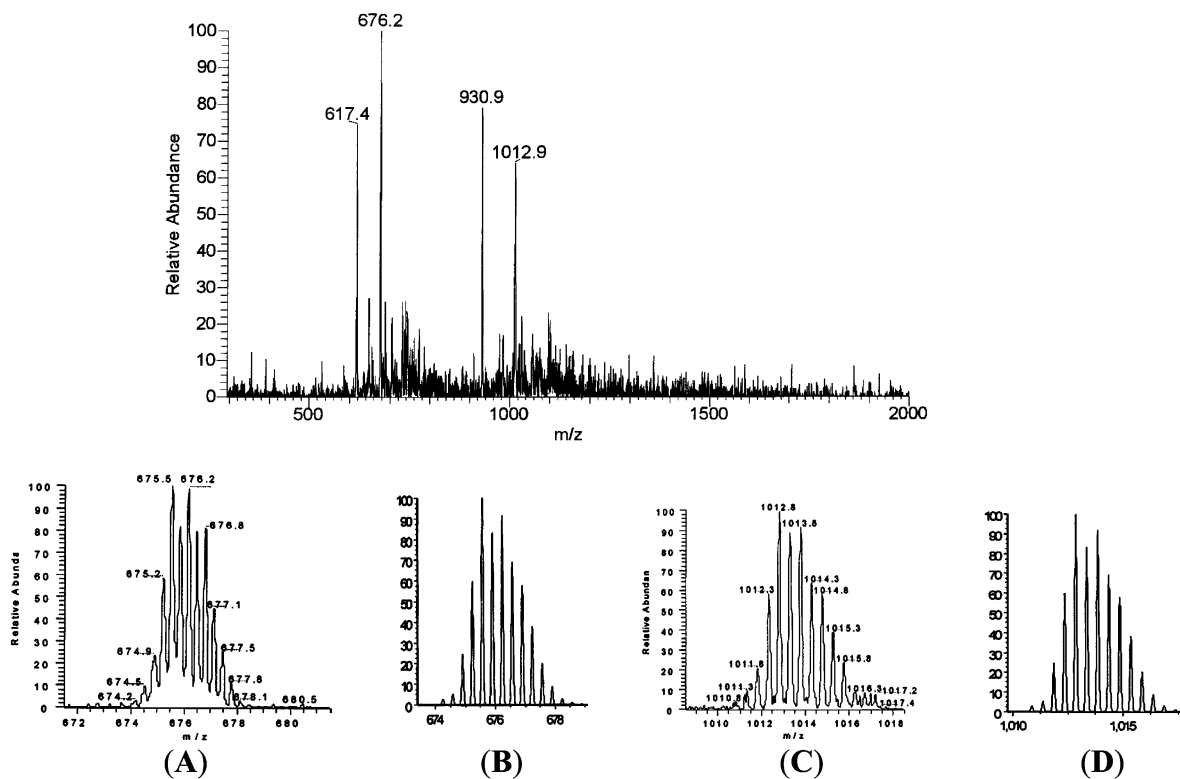


Figure 1. ESIMS spectrum measured 30 min after mixing of MP-11 with $cis\text{-}[Pd(en)(H_2O)_2]^{2+}$ in a molar ratio of 1:1 at room temperature and pH 1.44. (A) Measured m/z values separated by 0.3 m/z unit. (B) Isotope distribution pattern for $[C_{86}H_{123}FeN_{22}O_{21}S_2Pd+H^+]^{3+}$ calculated by IsoPro 3.0 program. (C) Measured m/z values separated by 0.5 m/z unit. (D) Isotope distribution pattern for $[C_{86}H_{123}FeN_{22}O_{21}S_2Pd]^{2+}$ calculated by IsoPro 3.0 program.

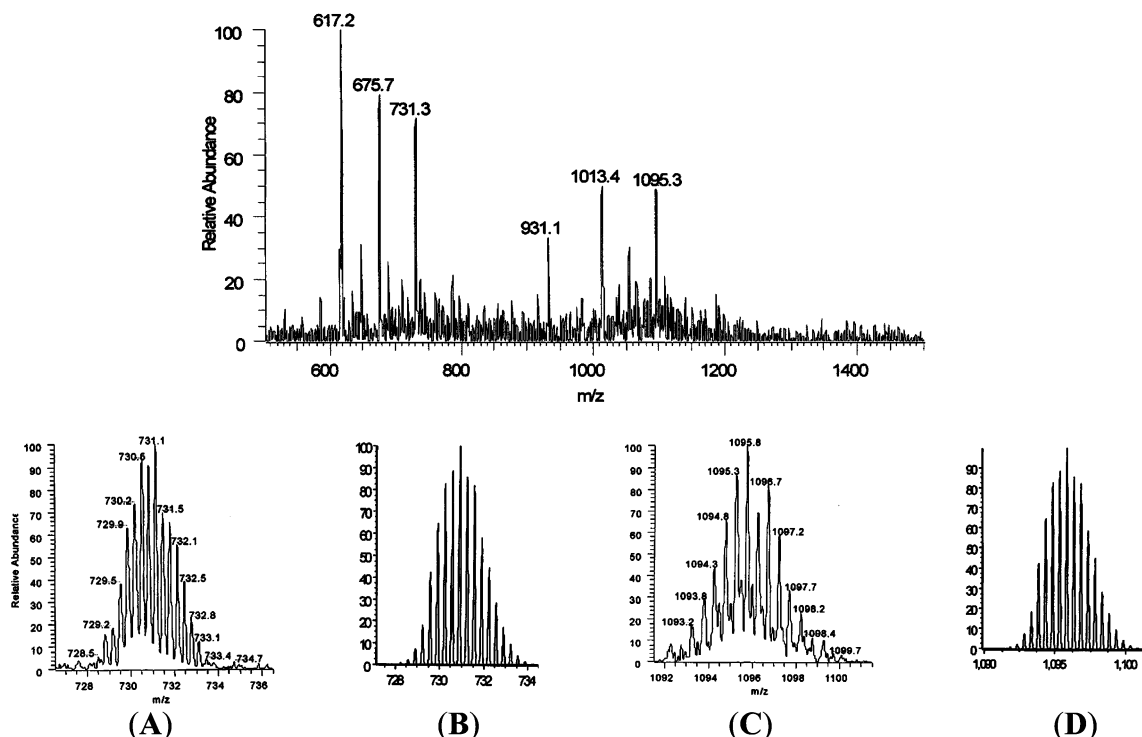


Figure 2. ESIMS spectrum measured 30 min after mixing of MP-11 with $cis\text{-}[Pd(en)(H_2O)_2]^{2+}$ in a molar ratio of 1:2 at room temperature and pH 1.44. (A) Measured m/z values separated by 0.3 m/z unit. (B) Isotope distribution pattern for $[C_{88}H_{130}FeN_{24}O_{21}S_2Pd_2]^{3+}$ calculated by IsoPro 3.0 program. (C) Measured m/z values separated by 0.5 m/z unit. (D) Isotope distribution pattern for $[C_{88}H_{130}FeN_{24}O_{21}S_2Pd_2-H^+]^{2+}$ calculated by IsoPro 3.0 program.

and 1012.9 exactly represent an identical species in which one $Pd(en)^{2+}$ anchors to the MP-11.

ESIMS was measured 30 min after mixing MP-11 with $cis\text{-}[Pd(en)(H_2O)_2]^{2+}$ in a molar ratio of 1:2 at room tem-

perature and pH 1.4. In comparison with Figure 1, two new abundant peaks at 731.3 and 1095.3 appeared in Figure 2. The isotopic peaks of 731.3 separated by 0.3 m/z unit correspond to a complex of $[C_{88}H_{130}FeN_{24}O_{21}S_2Pd_2]^{3+}$ in which

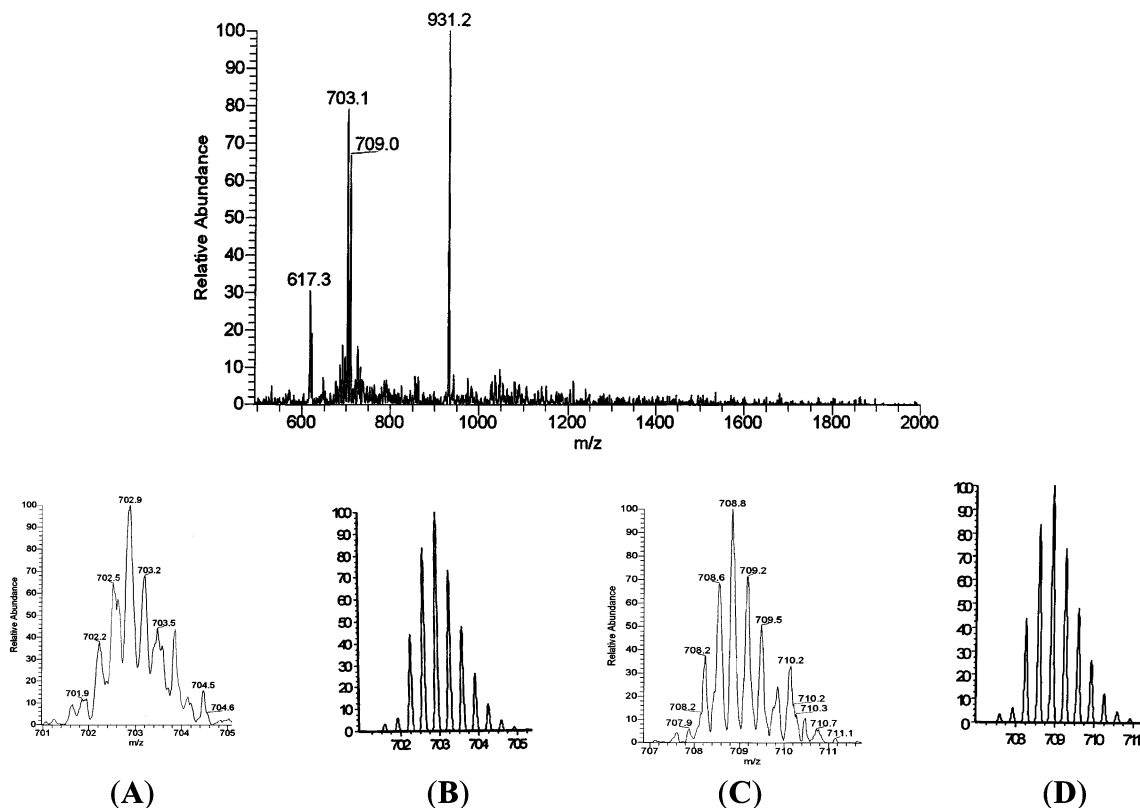


Figure 3. ESIMS spectrum measured 1 h after mixing of MP-11 with *cis*-[Pt(NH₃)₂(H₂O)₂]²⁺ in a molar ratio of 1: 2 at room temperature and pH 1.4. (A) Measured *m/z* values separated by 0.3 *m/z* values. (B) The isotopic distribution pattern for [C₈₄H₁₂₄FeN₂₂O₂₂S₂Pt]³⁺ calculated by IsoPro 3.0 program. (C) Measured *m/z* values separated by 0.3 *m/z* values. (D) The isotopic distribution pattern for [C₈₄H₁₂₆FeN₂₂O₂₃S₂Pt]³⁺ calculated by IsoPro 3.0 program.

two Pd(en)²⁺ coordinate to the MP-11 with calculated mass value of 2192.9. The isotopic peaks of 1095.3 are attributed to a double charged complex of [C₈₈H₁₂₉FeN₂₄O₂₁S₂Pd₂]²⁺, where two Pd(en)²⁺ anchor to the polypeptide, too. Again, the peaks at 731.3 and 1095.3 are related to the same species with different charges. The molecular mass, combined with isotopic peaks and simulation of MS spectra, successfully determined the composition of the species present in solution.

ESIMS Measurement for the Mixed Solution of *cis*-[Pt(NH₃)₂(H₂O)₂]²⁺ with MP-11. *cis*-[Pt(NH₃)₂(H₂O)₂]²⁺ was mixed with MP-11 in a molar ratio of 2: 1 at pH 1.4. The mixed solution was kept at room temperature for 1 h and then used in ESIMS measurements. As shown in Figure 3, the new peaks at 703.1 and 709.0 appeared in addition to peaks of 617.3 and 931.2. The isotopic peaks of 703.1 separated by 0.3 *m/z* unit (A) are in good agreement with [C₈₄H₁₂₄FeN₂₂O₂₂S₂Pt]³⁺(B), in which one [Pt(NH₃)₂(H₂O)]²⁺ coordinates to the MP-11. The isotopic peaks of 709.0 (C), combined with simulated distribution pattern (D), confirmed that species [C₈₄H₁₂₆FeN₂₂O₂₃S₂Pt]³⁺ is only different from the [C₈₄H₁₂₄FeN₂₂O₂₂S₂Pt]³⁺ by one H₂O molecule which coordinates to heme as an axial aqua ligand. The coordination of two [Pt(NH₃)₂(H₂O)]²⁺ to the MP-11 was also observed after 5 h of the mixed solution kept at room temperature. The peaks of 790.7 and 796.7, both separated by 0.3 *m/z* unit, are assigned as [C₈₄H₁₃₂FeN₂₄O₂₄S₂Pt₂]³⁺ and [C₈₄H₁₃₂-FeN₂₄O₂₄S₂Pt₂+H₂O]³⁺. It is evident that the ESIMS measurements are useful to determine the composition of the Pd(II)- and Pt(II)-bound MP-11. However, it is not known

at the current stage which is favorable anchoring site for Pd(II) and Pt(II) ions among the potential residues such as Val1, Lys3, Cys4, Cys7, and His8. The ability of MS/MS to sequence peptides encouraged us to apply this method to characterize the binding sites of Pd(II) and Pt(II) ions to the MP-11.

MS/MS Analysis. Thus far, the reported MS/MS method is mainly used for sequencing peptides or proteins, instead of *N*-terminal amino acid sequencing by Edman degradation,^{11,41–46} and has not yet been applied for the determination of metal binding site in peptides. This appears to be the first attempt to apply the MS/MS method to determine the binding site of Pd(II) and Pt(II) ions to MP-11. We choose the peak of 676.2³⁺ present in Figure 1 as a precursor ion. The relative collision energy was increased from 10% to 30%. The nomenclature used for the fragmentation pattern was based on conventional notation.^{47,48} The fragment ions are assigned a_{*n*}, b_{*n*}, c_{*n*} when the charges are retained by *N*-terminal fragments, and assigned x_{*n*}, y_{*n*}, z_{*n*} when the charges

- (41) Stenfors, C.; Hellman, U.; Silderring, J. *J. Biol. Chem.* **1997**, *272*, 5747.
- (42) Liu, T.; Shao, X. X.; Zeng, R.; Xia, Q. C. *J. Chromatogr. A* **1999**, *855*, 695.
- (43) Smith, R. D.; Loo, J. A.; Barinaga, C. J.; Edmonds, C. G.; Udseth, H. R. *J. Am. Soc. Mass Spectrom.* **1990**, *1*, 53.
- (44) Barinaga, C. J.; Edmonds, C. G.; Udseth, H. R.; Smith, R. D. *Rapid Commun. Mass Spectrom.* **1989**, *3*, 160.
- (45) Loo, J. A.; Edmonds, C. G.; Smith, R. D. *Science* **1990**, *248*, 201.
- (46) Loo, J. A.; Edmonds, C. G.; Smith, R. D. *Anal. Chem.* **1993**, *65*, 425.
- (47) Biemann, K.; Schible, H. A. *Science* **1987**, *237*, 992.
- (48) Roepstorff, P.; Fohlman, J. *J. Biomedic. Mass Spectrom.* **1984**, *11*, 601.

Table 1. MS/MS Analysis for $[\text{C}_{86}\text{H}_{124}\text{FeN}_{22}\text{O}_{21}\text{S}_2\text{Pd}]^{3+}$ (m/z 676.2)^a

assignment	m/z value	
	calculated	observed
b_2^+	228.1	228.1
b_3^+	356.2	355.3
b_4^+	459.2	459.1 (459.1)
b_5^+	530.3	530.5 (530.3)
b_6^+	658.3	658.5 (658.4)
$\text{b}_7^{2+}(\text{Pd})$ (b_7^+)	463.4 (761.3)	463.1 (760.9)
$\text{b}_7^{2+}(\text{Pd}+\text{H}_2\text{O})$	472.4	472.8
$\text{b}_8^{2+}(\text{Pd})$ (b_8^+)	532.0 (898.4)	531.3 (898.3)
$\text{b}_8^{2+}(\text{Pd} + \text{H}_2\text{O})$	541.0	540.5
$\text{b}_9^{2+}(\text{Pd})$ (b_9^+)	582.5 (999.5)	582.3 (999.1)
$\text{b}_9^{2+}(\text{Pd}+\text{H}_2\text{O})$	591.5	591.5
$\text{b}_{10}^{2+}(\text{Pd})$ (b_{10}^+)	632.0 (1098.5)	631.8 (1098.3)
$\text{b}_{10}^{2+}(\text{Pd}+\text{H}_2\text{O})$	641.0	640.3
y_2^+	247.1	246.8
y_3^+	348.2	348.1
y_4^+	485.2	485.2 (485.2)
$\text{y}_5^+(\text{Pd})$ (y_5^+)	752.7 (588.2)	752.7 (588.1)
$\text{y}_6^{2+}(\text{Pd})$ (y_6^+)	440.9 (716.3)	441.0 (716.7)
$\text{y}_6^{2+}(\text{Pd}+\text{H}_2\text{O})$	449.9	449.3
$\text{y}_7^{2+}(\text{Pd})$ (y_7^+)	476.4 (787.3)	476.5 (787.3)
$\text{y}_7^{2+}(\text{Pd}+\text{H}_2\text{O})$	485.4	485.2
$\text{y}_8^{2+}(\text{Pd})$ ($\text{y}_8^++\text{H}_2\text{O}$)	527.9 (908.3)	528.0 (908.3)
$\text{y}_8^{2+}(\text{Pd}+\text{H}_2\text{O})$	536.9	537.0
$\text{y}_9^{2+}(\text{Pd})$ (y_9^+)	592.0 (1018.4)	592.0 (1017.9)
$\text{y}_9^{2+}(\text{Pd}+\text{H}_2\text{O})$	601.0	601.3
$\text{y}_{10}^{2+}(\text{Pd})$	656.0	656.0
$\text{y}_{10}^{2+}(\text{Pd}+\text{H}_2\text{O})$	665.0	665.2

^a Pd represents the $\text{Pd}(\text{en})^{2+}$ moiety. The assignments and m/z values for the fragment ions generated from free MP-11 are listed in parentheses.

Table 2. MS/MS Analysis for $[\text{C}_{88}\text{H}_{130}\text{FeN}_{24}\text{O}_{21}\text{S}_2\text{Pd}_2]^{3+}$ (m/z 731.3)^a

assignment	m/z value	
	calculated	observed
b_2^+	228.1	227.9
b_3^+	356.2	356.3
$\text{b}_4^+(\text{Pd})$	623.7	623.8
$\text{b}_5^{2+}(\text{Pd})$	347.9	348.1
$\text{b}_5^{2+}(\text{Pd} + \text{H}_2\text{O})$	356.9	356.3
$\text{b}_6^+(\text{Pd})$	822.8	822.2
$\text{b}_7^{2+}(2\text{Pd}+\text{OH})$	554.7	554.7
$\text{b}_7^{2+}(2\text{Pd}+\text{OH}+\text{H}_2\text{O})$	563.7	563.8
$\text{b}_8^{2+}(2\text{Pd}+\text{OH})$	623.2	623.8
$\text{b}_8^{2+}(2\text{Pd}+\text{OH}+\text{H}_2\text{O})$	632.2	632.3
$\text{b}_9^{2+}(2\text{Pd}+\text{OH})$	673.7	673.5
$\text{b}_9^{2+}(2\text{Pd}+\text{OH}+\text{H}_2\text{O})$	682.7	682.3
$\text{b}_{10}^{2+}(2\text{Pd}+\text{OH})$	723.3	723.0
$\text{b}_{10}^{2+}(2\text{Pd}+\text{OH}+\text{H}_2\text{O})$	732.3	731.6
y_3^+	348.2	348.1
y_4^+	485.2	485.1
$\text{y}_5^+(\text{Pd})$	752.7	752.5
$\text{y}_6^+(\text{Pd})$	880.8	880.7
$\text{y}_7^+(\text{Pd})$	951.8	951.3
$\text{y}_8^{2+}(2\text{Pd}+\text{H}_2\text{O})$	619.2	619.4
$\text{y}_9^{3+}(2\text{Pd})$	449.8	450.3
$\text{y}_9^{3+}(2\text{Pd}+2\text{H}_2\text{O})$	461.8	461.1
$\text{y}_{10}^{2+}(2\text{Pd}+2\text{H}_2\text{O})$	756.2	756.3

^a Pd represents the $\text{Pd}(\text{en})^{2+}$ moiety.

are retained by C-terminal fragments. The binding sites are determined by interpreting the MS/MS spectra. Only b_n and y_n were characterized because they are the most common fragments that have greater stability toward further dissociation.⁴⁹ Tables 1–3 show only the successive fragment ions b_n and y_n . A superscript refers to the charge of the ion. In

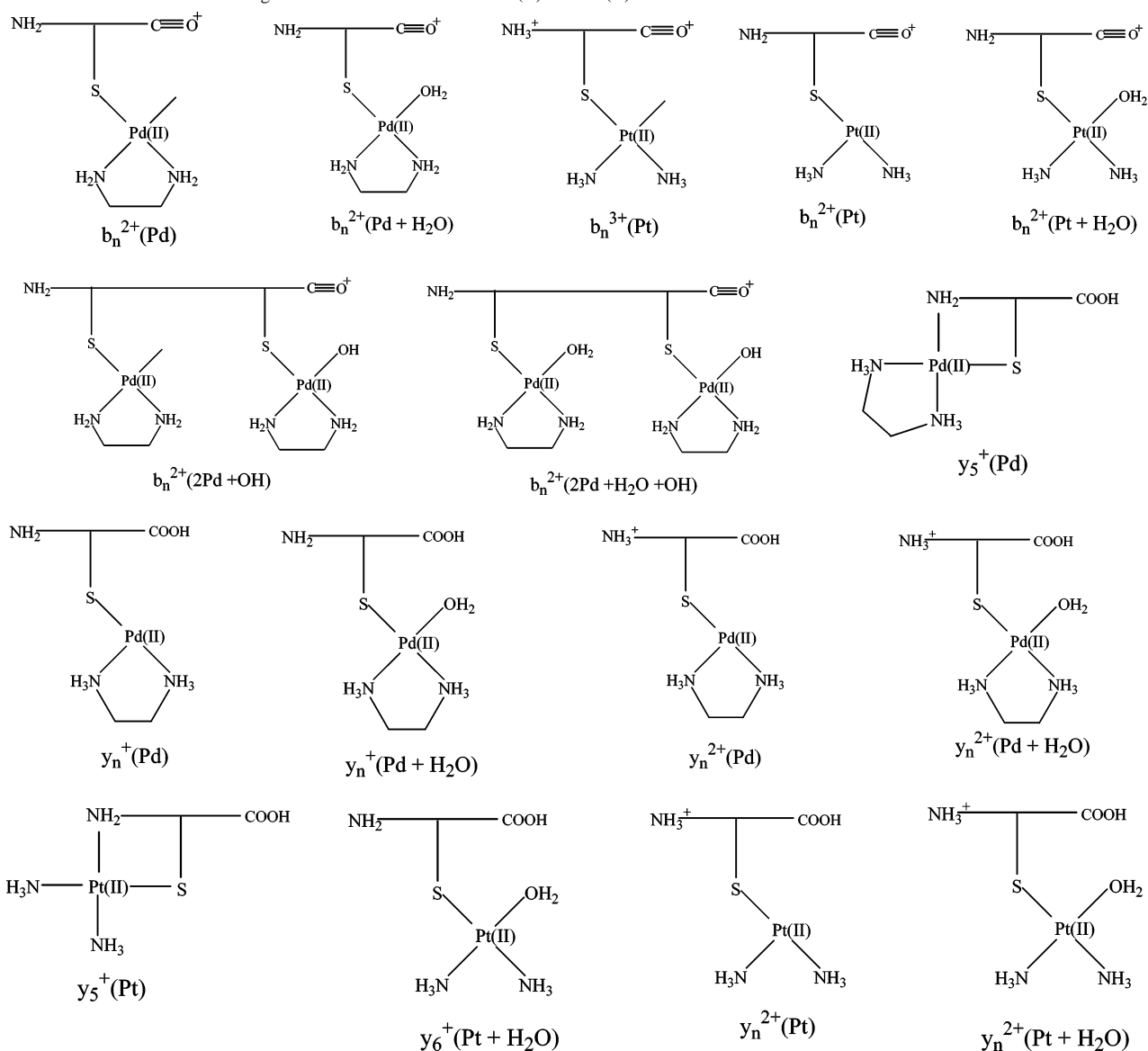
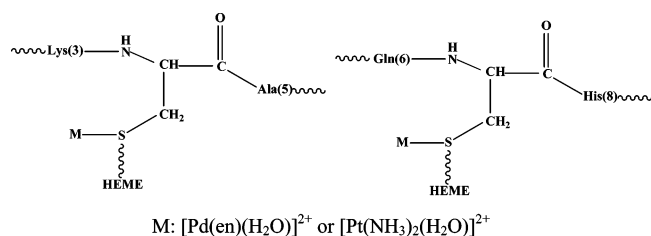
Table 3. MS/MS Analysis for $[\text{C}_{84}\text{H}_{124}\text{FeN}_{22}\text{O}_{22}\text{S}_2\text{Pt}]^{3+}$ (m/z 703.1)^a

assignment	m/z value	
	calculated	observed
b_2^+	228.1	228.1
$\text{b}_3^+-\text{H}_2\text{O}$	338.2	338.2
b_4^+	459.2	459.0
$\text{b}_4^++\text{H}_2\text{O}$	477.2	476.6
b_5^+	530.3	530.0
$\text{b}_5^++\text{H}_2\text{O}$	548.3	548.3
b_6^+	658.3	658.2
$\text{b}_7^{3+}(\text{Pt})$	330.1	330.1
$\text{b}_8^{2+}(\text{Pt})$	563.2	562.6
$\text{b}_8^{2+}(\text{Pt}+\text{H}_2\text{O})$	572.2	572.2
$\text{b}_9^{3+}(\text{Pt})$	409.5	410.0
$\text{b}_9^{2+}(\text{Pt})$	613.8	613.9
$\text{b}_9^{2+}(\text{Pt}+\text{H}_2\text{O})$	622.8	622.7
$\text{b}_{10}^{3+}(\text{Pt})$	442.5	441.9
$\text{b}_{10}^{2+}(\text{Pt})$	663.3	664.0
$\text{b}_{10}^{2+}(\text{Pt}+\text{H}_2\text{O})$	672.3	672.5
y_3^+	348.2	348.0
y_4^+	485.2	485.3
$\text{y}_5^+(\text{Pt})$	816.3	816.6
$\text{y}_5^+(\text{Pt}+\text{H}_2\text{O})$	834.3	833.9
$\text{y}_6^+(\text{Pt}+\text{H}_2\text{O})$	961.4	961.9
$\text{y}_7^{3+}(\text{Pt})$	338.8	338.2
$\text{y}_7^{2+}(\text{Pt})$	507.7	508.5
$\text{y}_8^{3+}(\text{Pt})$	373.1	373.2
$\text{y}_9^{2+}(\text{Pt}+\text{H}_2\text{O})$	632.3	632.6
$\text{y}_{10}^{2+}(\text{Pd})$	687.3	687.0

^a Pt represents the $\text{Pt}(\text{NH}_3)_2^{2+}$ moiety.

the MS/MS spectra of free MP-11 for the 931^{2+} ion, the successive N-terminal fragment ions b_4 – b_{10} and C-terminal fragment ions y_4 – y_9 exactly match the backbone sequence of MP-11 without heme involved and are also listed in Table 1 for comparison. This means that the heme is broken down from MP-11 in the MS/MS fragmentation process and the backbone sequence of the MP-11 provides a convenience for determining binding sites of Pd(II) and Pt(II) to the MP-11. Compared to the conventional MS/MS analysis of peptide backbones, it should be mentioned in this study that the MS/MS spectra for the free MP-11 as well as Pd(II)- and Pt(II)-bound MP-11 are rather poor. There are several factors affecting the spectral quality. In the MS/MS fragmentation of free MP-11, besides free heme ion (617) and the fragment ions from the MP-11 backbone observed, the fragment ions with heme also appeared. It makes the MS/MS spectra complicated. In the MS/MS fragmentation for Pd(II)- and Pt(II)-bound MP-11, more complication arose from decreasing sensitivity of MS/MS spectra and increasing varieties of fragment ions. Therefore, we carried out MS/MS fragmentation several times for a given precursor ion. The data listed in Tables 1–3 are the average values. Some representatives of Pd(II)- and Pt(II)-involved fragment ions assigned in the tables are exhibited in Chart 2. These fragment ions seem to be generated by cleavage of thioether linkages and peptide bonds of the MP-11 backbone. Table 1 shows that the N-terminal fragment ions from b_7 to b_{10} contain one $\text{Pd}(\text{en})^{2+}$ ion anchored to the backbone of MP-11. Again, the C-terminal fragment ions from y_5 to y_{10} contain one $\text{Pd}(\text{en})^{2+}$ ion attached, too. As seen from Chart 1, the fragment ions b_7 and y_5 are respectively obtained by cleavage of peptide bond at C- and N-terminals of Cys7 in the MS/MS fragmentation process. Therefore, the results

(49) Tang, X. J.; Thibault, P.; Boyd, K. *Anal. Chem.* **1993**, *65*, 2824.

Chart 2. The MS/MS Induced Fragmental Ions Generated from Pd(II)- and Pt(II)-Bound MP-11**Chart 3.** Anchor of $\text{cis-}[\text{Pd}(\text{en})(\text{H}_2\text{O})_2]^{2+}$ and $\text{cis-}[\text{Pt}(\text{NH}_3)_2(\text{H}_2\text{O})_2]^{2+}$ to MP-11

obtained by MS/MS analysis from both *N*- and *C*-terminals for Pd(II)-anchored MP-11 reveal that the Pd(II) ion, occurring as $\text{Pd}(\text{en})^{2+}$, anchors to the side chain of Cys7, as described in Chart 3. On the basis of the composition and charge of $[\text{C}_{86}\text{H}_{123}\text{FeN}_{22}\text{O}_{21}\text{S}_2\text{Pd}]^{2+}$, the fourth coordination site of Pd(II) is occupied by the deprotonated amide nitrogen of His8.^{31,32} The Pd(II)-induced deprotonation of the amide nitrogen is especially favorable when the Pd(II) is already anchored to the side chain.^{50,51} It is concluded that the Pd(II) ion prefers initially binding to the side chain of

Cys7. The MS/MS spectrum was also recorded for $[\text{C}_{88}\text{H}_{130}\text{FeN}_{24}\text{O}_{21}\text{S}_2\text{Pd}_2]^{3+}$ (m/z 731.1) in Figure 2. Table 2 shows the *N*-terminal fragment ions b_2 – b_{10} and the *C*-terminal fragment ions y_3 – y_{10} . The fragment ions from b_2 to b_3 have no Pd(II) ion involved. One $\text{Pd}(\text{en})^{2+}$ ion is contained from b_4 to b_6 . The fragment ions from b_7 to b_{10} contain two $\text{Pd}(\text{en})^{2+}$ ions. Again, the fragment ions from y_5 to y_7 with one $\text{Pd}(\text{en})^{2+}$ and from y_8 to y_{10} with two $\text{Pd}(\text{en})^{2+}$ ions were observed. The fragment ions b_4 and y_8 are created by the cleavage of *C*- and *N*-terminals of Cys4, and the fragment ions b_7 and y_5 formed by scission of *C*- and *N*-terminals of Cys7 during the MS/MS fragmentation process. It is evident that Cys4 is the second binding site of Pd(II) ion to the MP-11 in addition to Cys7, as exhibited in Chart 3. Therefore, when $\text{Pd}(\text{en})(\text{H}_2\text{O})_2^{2+}$ is mixed with MP-11 in equimolar or double-molar ratio, Cys7 is the preferred anchoring residue and Cys4 is the next choice for binding.

(50) Sigel, H.; Martin, R. B. *Chem. Rev.* **1982**, 385.(51) Sovago, I.; Martin, R. B. *J. Inorg. Nucl. Chem.* **1981**, 43, 425.

The MS/MS spectrum was also recorded for the $[C_{84}H_{124}FeN_{22}O_{22}S_2Pt]^{3+}$ (m/z 703.1) in Figure 3. The successive *N*-terminal fragment ions b_2 – b_{10} and *C*-terminal fragment ions y_3 – y_{10} were detected. The *N*-terminal fragment ions from b_7 to b_{10} contain one $Pt(NH_3)_2^{2+}$ ion attached to the backbone of MP-11. The *C*-terminal fragment ions from y_5 to y_{10} also contain one $Pt(NH_3)_2^{2+}$. Again, both *N*- and *C*-terminal MS/MS analyses for the $Pt(NH_3)_2^{2+}$ -anchored MP-11 prove that the Pt(II) ion binds to the side chain of Cys7. According to the composition and charge of $[C_{84}H_{124}FeN_{22}O_{22}S_2Pt]^{3+}$ and $[C_{84}H_{126}FeN_{22}O_{23}S_2Pt]^{3+}$, it seems that the Pt(II), as $[Pt(NH_3)_2(H_2O)]^{2+}$, anchors to the side chain of MP-11, as shown in Chart 3. One extra H_2O in the $[C_{84}H_{126}FeN_{22}O_{23}S_2Pt]^{3+}$, as an axial ligand, coordinates to Fe(III). The results obtained from Pd(II) and Pt(II) complexes are consistent. Therefore, the regioselectivity for anchoring of the Pd(II) and Pt(II) to the MP-11 is probably governed by the local environment around Cys7 and Cys4. In previous studies,^{31,32} it was shown that the hydrogen bonding was formed between protonated imidazole nitrogen of His8 and carbonyl oxygen of amino acid residue downstream of His8. Therefore, the regioselectivity seems to be relative to the side chain of His8. The hydrogen bonding makes the side chain of His8 apart from Cys7. As a result, Cys7 is more exposed and more favorable for the anchoring by Pd(II) and Pt(II) complexes.

Pd(II)- and Pt(II)-Mediated Cleavage of the His8–Thr9 Bond in MP-11. *cis*- $[Pd(en)(H_2O)_2]^{2+}$ or *cis*- $[Pt(NH_3)_2(H_2O)_2]^{2+}$ was in two molar excess mixed with MP-11 at pH 1.44, and the mixed solution was incubated at 40 °C for 2 or 3 days. Because the precipitation occurred during the incubation, we measured the ESIMS occasionally only after centrifugation of the digestion solution. A peak at 348 appeared and increased with time. This peak is attributed to a cleaved tripeptide of Thr–Val–Glu that is further confirmed by MS/MS analysis, with observed fragment ions: b_1^+ 102.1, y_1^+ 148.0, a_2^+ 173.0, b_2^+ 201.1, y_2^+ 247.1. These results indicated that *cis*- $[Pd(en)(H_2O)_2]^{2+}$ and *cis*- $[Pt(NH_3)_2(H_2O)_2]^{2+}$ have the same cleaved site of His8–Thr9 bond in this new finding. This pattern of cleavage is the same as that observed in cytochrome *c*.^{28,32} Although it was recently reported that *cis*- $[Pt(en)(H_2O)_2]^{2+}$ and $[Pd(H_2O)_4]^{2+}$ have different behavior in cleavage of methionine and histidine-containing peptides and myoglobin,³⁸ in fact, similarity in cleavage of peptide bond by the chemically similar Pd(II) and Pt(II) ions was also reported. In a previous study done by Kostić and Zhu,¹⁷ *cis*- $[Pd(en)(H_2O)_2]^{2+}$, $[Pd(H_2O)_4]^{2+}$, $PtCl_4^{2-}$, and *cis*- $[Pt(en)(H_2O)_2]^{2+}$ have the same cleaved site for cleavage of dipeptides, though the hydrolytic rates are different. Similar to cleavage of peptide bond by *cis*- $[Pd(en)(H_2O)_2]^{2+}$, the second peptide bond upstream from methionine anchored by *cis*- $[Pt(NH_3)_2(H_2O)_2]^{2+}$ was also cleaved.³⁷ Therefore, the similarity and difference in hydro-

lytic selectivity for the chemically similar Pd(II) and Pt(II) ions are still open for gaining an insight into investigation. The similarity in *cis*- $[Pd(en)(H_2O)_2]^{2+}$ and *cis*- $[Pt(NH_3)_2(H_2O)_2]^{2+}$ -mediated cleavage of MP-11 may be associated with the special sequence of Cys7–His8 in MP-11. Recently, it was reported that simple $ZnCl_2$ cleaved the peptide bond preceding Ser and Thr in dipeptides.¹⁶ Similar to Co(II) complexes,⁵ the $ZnCl_2$ mimics aminopeptidase. From previous study of Pd(II)-mediated cleavage of myoglobin done by Kostić and Zhu³³ and our recent study of myoglobin cleavage with $CuCl_2$, it was shown that the peptide bond preceding Thr95, which is second peptide bond downstream from His93 anchored by the Pd(II) and Cu(II) ions, was also cleaved in addition to major Gln91–Ser92 bond cleavage. These results indicated that the OH group in Thr95 may assist cleavage of the peptide bond and the anchoring of metal ions to amino acid residue preceding the Thr95 is not required for the cleavage. As far as the *cis*- $[Pd(en)(H_2O)_2]^{2+}$ and *cis*- $[Pt(NH_3)_2(H_2O)_2]^{2+}$ -mediated cleavage of the His8–Thr9 bond in MP-11 is concerned, in previous and our recent investigation for tripeptide of CH_3CO -CysMe–His–Gly(or Ala), that was taken as a mimic for cytochrome *c* cleavage with Pd(II) complexes, the second peptide bond downstream from *s*-methylcysteine was cleaved.^{31,32} The site of cleavage is the same as that in MP-11 and cytochrome *c*. This means that the cleavage reaction in MP-11 and cytochrome *c* is not governed by the threonine and is sequence-specific. The Cys–His sequence is required for the cleavage.^{31,32} The threonine may be expected to assist the cleavage reaction. What role the threonine plays in Cyt *c* cleavage needs further investigation after understanding the binding site of Pd(II) and Pt(II) to MP-11 and Cyt *c*. In short, this MS/MS study provides a direct evidence for the initial binding site of *cis*- $[Pd(en)(H_2O)_2]^{2+}$ and *cis*- $[Pt(NH_3)_2(H_2O)_2]^{2+}$ toward MP-11.

Conclusion

This work represents the first MS/MS study for the metal binding sites in peptides. The *cis*- $[Pd(en)(H_2O)_2]^{2+}$ and *cis*- $[Pt(NH_3)_2(H_2O)_2]^{2+}$ prefer initially to anchor to the side chain of Cys7 in MP-11. The two complexes cleaved the same His8–Thr9 bond of the MP-11. These results add additional support that the Pd(II)-mediated cleavage of the His18–Thr19 bond in cytochrome *c* is associated with the initial anchoring of Pd(II) to the side chain of Cys17, rather than to the side chain of His18. This study proves that ESIMS and MS/MS analysis are powerful techniques for determining the composition and the binding sites for metal-bound peptides.

Acknowledgment. This work was supported by the National Natural Science Foundation of China (20271027 and 20231010).

IC034491A